Molecular Phylogenetics and Evolution 139 (2019) 106536

Contents lists available at ScienceDirect

Molecular Phylogenetics and Evolution

journal homepage: www.elsevier.com/locate/ympev

Complex evolutionary history of the American Rubyspot damselfly, *Hetaerina americana* (Odonata): Evidence of cryptic speciation

Yesenia Margarita Vega-Sánchez[a], Luis Felipe Mendoza-Cuenca[b], Antonio González-Rodríguez[a,*]

[a] Instituto de Investigaciones en Ecosistemas y Sustentabilidad, Universidad Nacional Autónoma de México, Antigua carretera a Pátzcuaro #8701, Morelia, Michoacán 58190, Mexico

[b] Facultad de Biología, Universidad Michoacana de San Nicolás de Hidalgo, Av. Francisco J. Múgica, Morelia, Michoacán 58030. Mexico

ARTICLE INFO

Keywords:
Calopterygidae
Mitonuclear discordance
Genetic divergence
Caudal appendages
Reproductive isolation, nonecological speciation

ABSTRACT

Analyzing the magnitude and distribution of genetic variation within and among populations allows for hypothesis testing about historical demographic size changes, secondary contacts, refugia, and speciation patterns. Species distribution and genetic structure are greatly influenced by the complex life cycle and behavior of odonates. *Hetaerina americana* has been widely used as a model system in behavioral studies, but its population genetic structure has not been analyzed, except for a single study that included only three populations but identified the presence of markedly differentiated genetic groups, suggesting the existence of cryptic species. Here, we tested this hypothesis by assessing throughout the distribution range of *H. americana* the patterns of genetic and morphological variation in the male caudal appendages, due to the great importance of these structures in mate recognition. As molecular markers we used sequences of the mitochondrial cytochrome oxidase I (COI) gene and the nuclear internal transcribed spacer (ITS) region, as well as six nuclear microsatellites. We found very high population genetic differentiation ($\Phi_{ST} > 0.51$) in the three sets of markers but with strong mitonuclear discordance. A neutrality test suggested that the mitochondrial genome might be under purifying selection in association to climatic variables (temperature seasonality). The assignment of individuals to nuclear genetic groups showed little admixture and complete congruence with morphological differentiation in the male caudal appendages. Hence, the results suggest that *H. americana* represents at least two different cryptic species which are isolated reproductively.

1. Introduction

The current distribution of species is a result of several historical and contemporary factors, including dispersal, vicariance and gene flow (Avise, 2000). Analyzing how the distribution of evolutionary lineages changes over time allows us to test hypotheses about historical demographic size changes, secondary contacts, refugia and speciation patterns (Futuyma and Kirkpatrick, 2017). In odonates, understanding the factors that have shaped species distribution and genetic structure may be difficult because of their complex life cycle and behavior. For example, previous studies in this insect group have shown that some species are constituted by a single panmictic population at a global scale (Troast et al., 2016), while others show isolation by distance within few kilometers (Watts et al., 2004). These differences seem to be related to the dispersal capacity of the individuals of each species as well as to their territorial or migratory behavior. Also, the effects of particular physical barriers and the Quaternary glacial cycles have also been documented for some species (Callahan and McPeek, 2016; Jones and Jordan, 2015).

Genetic divergence can also be related to the evolution of reproductive isolation barriers. In odonates, the most common pre-zygotic barriers are sexual and mechanical or sensory isolation (Battin, 1993; Sánchez-Guillén et al., 2014a, 2014b; Svensson and Waller, 2013). Sexual isolation has been associated with the coloration of individuals, such as in *Calopteryx* (Svensson et al., 2016; Tynkkynen et al., 2008), *Mnais* (Hayashi et al., 2005) and *Argia* (Nava-Bolaños et al., 2016), in which differences in wing and body coloration result in assortative mating, leading to genetic differentiation even among populations within species (Svensson et al., 2004). In turn, mechanical or sensory isolation is mainly related to the morphological configuration of clasping structures in males and the prothorax or head in females. The clasping structures (i.e. the caudal appendages) are structures found at the end of the abdomen of the males and used to grasp females and form the tandem position during copulation (Corbet, 1962). It has

* Corresponding author.
E-mail addresses: yvega@cieco.unam.mx (Y.M. Vega-Sánchez), agrodrig@iies.unam.mx (A. González-Rodríguez).

https://doi.org/10.1016/j.ympev.2019.106536
Received 6 March 2019; Received in revised form 21 May 2019; Accepted 14 June 2019
Available online 15 June 2019

been suggested that besides the mechanical compatibility, there must be tactile stimuli for the female to accept to copulate (Barnard et al., 2017). The shape of the caudal appendages is well known to be species-specific in several genera of zygoptera (Barnard et al., 2017; Sánchez-Guillén et al., 2014b), but the role of intraspecific variation of these structures on mating patterns, genetic differentiation and incipient speciation processes has been barely analyzed (Barnard et al., 2017).

Despite that existence of more than 5000 species of odonates, to date the analyses of genetic differentiation and phylogeographic patterns are limited to a few species, mostly Palearctic and Nearctic species (Ferreira et al., 2016; Kohli et al., 2018; Swaegers et al., 2014; but see Feindt et al., 2014; Fincke et al., 2018; Sánchez-Herrera et al., 2010). In this study, we focused on *Hetaerina americana* (Calopterygidae), a broadly distributed species with a range from southeastern Canada to Nicaragua. Species of *Hetaerina* (commonly known as rubyspots), are characterized by the presence of a red spot at the base of the wings of male individuals and a territorial behavior. Most rubyspots are found along the neotropical region, with the highest species richness being found in South America (Garrison, 1990). Species identification within this genus has been problematic since many of them are very similar in wing and body coloration, body size, and are usually sympatric. Therefore, the main traits that allows an unambiguous species recognition are the morphology of the male caudal appendages (Garrison, 1990).

Hetaerina americana has been reported to occur in a variety of habitats, from temperate to tropical forests, and frequently is the most abundant species when it is in sympatry with other rubyspot species. *Hetaerina americana* is morphologically variable in the shape of the caudal appendages of the males and other traits such as the presence or absence of the pterostigma (i.e. a specialized colored cell in the outer wings, related to gliding control during flight) and the relative size of the red spots in the wings. Due to this variability, several synonymous taxa have been described (for example, *H. pseudoamericana, H. texana, H. californica,* etc.) (Garrison, 1990).

Hetaerina americana has been widely used as a model system in behavioral studies due to its complex mating system (Contreras-Garduño et al., 2008; Grether, 1996; Raihani et al., 2008). Males are territorial and display a lekking behavior (Córdoba-Aguilar et al., 2009), in which groups of males defend territories in the riverbanks and perform flying displays while females visit these areas to mate and do not receive other resources from males (nuptial gifts, oviposition sites). However, the population genetic structure of this species has not been studied and therefore no information is available regarding gene flow patterns and population history throughout its range. The only previous study was performed by Vega-Sánchez (2013), in which three widely separated populations of the species were analyzed using nuclear DNA sequences of the internal transcribed spacer 1, the 5.8S ribosomal RNA gene and the transcribed spacer internal 2 (ITS1-5.8S-ITS2) region. The populations analyzed were from Colorado in USA, and from Veracruz and Oaxaca in Mexico. The results showed a very high genetic differentiation among the three populations ($\Phi_{ST} > 0.60$) and, remarkably, the presence of two similarly highly differentiated sets of individuals within the Veracruz population (Vega-Sánchez, 2013). Even though geographic isolation may partially explain these results, the considerable genetic differentiation among individuals within the Veracruz population indicates that other mechanisms of genetic isolation may be operating at a local level and suggesting that *H. americana* may be a complex of cryptic species. To test this hypothesis, in this study we performed a detailed phylogeographic and genetic structure analysis of *H. americana* throughout its distribution range using sequences of a fragment of the mitochondrial gene cytochrome oxidase I (COI) and the nuclear ITS1-5.8S-ITS2 region, as well as six nuclear microsatellites. Additionally, we employed geometric morphometric techniques to analyze and compare the shape variation of the male caudal appendages. The specific questions addressed were (i) what are the patterns of population genetic structure in *H. americana* throughout its distribution range? (ii) is the morphological variation of the male caudal appendages congruent with genetic differentiation patterns? (iii) does the evidence support the cryptic speciation hypothesis in *H. americana*?

2. Materials and methods

2.1. Sampling

Two hundred and twenty adult individuals of *H. americana* were directly collected or obtained through donations, representing a total of 31 localities (Supplementary Table 1), from Guatemala to the United States, covering most of its distribution range.

2.2. DNA extraction, amplification, sequencing and genotyping

Genomic DNA was isolated from thoracic muscle with the Pure Link Genomic DNA Mini Kit (Invitrogen®) following the protocol of the manufacturer. A fragment of the cytochrome oxidase I (COI; 658 pb) gene was amplified using the ODO_HCO2198d and ODO_LCO1490d primers (Dijkstra et al., 2014). We also amplified the nuclear region of the internal transcribed spacers (ITS1 and ITS2) and the 5.8S coding sequence (hereafter referred to as "ITS"; 600 pb) for a subsample of eleven populations, using the primers 18S rDNA (Weekers et al., 2001) and 28R1 (Dumont et al., 2010). Reactions were prepared on a final volume of 25 μL using 10 μL of *Taq* PCR Master Mix Kit 2x (Qiagen®), 1 μL of each primer (13 pmol/μL) and 1 μL of template DNA (10 ng/μL). The amplification protocol consisted of an initial denaturation step of three minutes at 94 °C, followed by 30–35 cycles of one minute at 94 °C, one minute at 50–58 °C and one minute at 72 °C, with a final extension at 72 °C for three minutes. The annealing temperature and the number of cycles depended on the DNA quality, see Supplementary Table 2 for details. PCR products were sent for sequencing to Macrogen Company (Rockville, MD, USA) using ODO_LCO1490d primer for the COI region and 18S primer for the nuclear region. Additionally, six nuclear microsatellite loci previously characterized for *H. americana* (Anderson and Grether, 2013) were amplified (H3, H8, H11, H15, H17 and H22) using a final volume of 10 μL with 5 μL of Platinum Multiplex PCR Master Mix (Applied Biosystems®), 1 μL of each primer (13 pmol/μL) and 1 μL of template DNA (10 ng/μL). We grouped the primers in multiplex reactions; the first group was formed by primer pairs H8, H11 and H22; the second group by H15 and H17, and the H3 locus was amplified alone. The amplification protocol consisted of an initial denaturation step of three minutes at 94 °C followed by 30–35 cycles of one minute at 94 °C, one minute at 54–58 °C and one minute at 72 °C, with a final extension at 72 °C for three minutes (see Supplementary Table 2 for details). The fragments were analyzed on an ABI 3300 Avant-PRIMS sequencer (Applied Biosystems®) and the size of the fragments was determined in Peak Scanner v. 2.0 (Applied Biosystems®) using as reference of size the marker Liz GeneScan 600 (Qiagen®).

2.3. Analyses of DNA sequences

Both sets of sequences, COI and ITS, were manually aligned using MEGAX (Kumar et al., 2018). For the COI alignment we added 11H. *americana* sequences obtained from the barcode of life data System (BOLD), which came from five localities in the United States and from three localities in Canada (Supplementary Table 1). For the ITS, sequences were first analyzed with the phase algorithm in DnaSP v. 5 (Librado and Rozas, 2009) to reconstruct haplotypes, and were tested for recombination using IMgc (Woerner et al., 2007). Haplotype (Hd) and nucleotide (π) diversity, the rarefacted haplotype richness (h) and Tajima's D and Fu's Fs were obtained for each population using DnaSP v. 5 (Librado and Rozas, 2009). For some of these analyses, populations with small sample sizes were grouped with others according to their

geographic proximity (see Supplementary Tables 2 and 3). Additionally, the overall average rate of synonymous (d_S) and non-synonymous (d_N) mutations in the COI sequences were estimated using the Nei and Gojobori's (1986) method with the Jukes and Cantor (1969) correction and both estimates were compared with a Z-test, to evaluate the null hypothesis of strict neutrality of this gene ($d_S = d_N$). The variance of the difference between the two estimates was computed using the bootstrap method with 1000 replicates. The MEGAX software was used for this analysis.

Population genetic differentiation was evaluated with analyses of molecular variance (AMOVA), using matrices of pairwise differences among haplotypes. Statistical significance of the differentiation estimates was determined with 10,000 permutations. These analyses were performed for individuals grouped according to their population of origin and grouped according to haplogroups (see Results section). The Arlequin v. 3.5 software (Excoffier and Lischer, 2010) was used for these analyses.

Haplotype networks were constructed for both COI and ITS datasets based on statistical parsimony in TCS v. 1.2.1 (Clement et al., 2000), using a connection limit of 90% probability. Additionally, phylogenetic relationships among haplotypes were analyzed using a Bayesian approach. Both datasets were analyzed in JModelTest v. 2.1.6 (Darriba et al., 2012) to determine the appropriate substitution model using the Bayesian Information Criterion (BIC). Then, phylogenetic relationships were estimated in MrBayes v. 3.2 (Ronquist et al., 2012) based on the GTR + G + I substitution model for COI and GTR + G for ITS. For each data set, two runs of 50 million generations were made, with trees sampled every 1000 generations. The convergence of the runs was evaluated through examination of ESS values in Tracer v. 1.7.0 (Rambaut et al., 2018). The initial 10% of reconstructions were discarded as burn-in to obtain a consensus tree. The tree was visualized in FigTree v. 1.4.3 (http://tree.bio.ed.ac.uk/software/figtree/). As outgroups, sequences of three other *Hetaerina* species (*H. laesa*, *H. sanguinea* and *H. titia*) were included in the COI phylogeny, of which the first two were obtained from GenBank and the third was generated for this study using the methods described above. In the case of the ITS phylogeny, we obtained sequences for *H. cruentata*, *H. medinai* and *H. titia* from GenBank (Supplementary Table 1).

For the ITS dataset, we estimated the divergence times among haplotypes with a Bayesian approach in BEAST v. 2.5 (Bouckaert et al., 2014) using the GTR + I + G model of molecular evolution, under an uncorrelated lognormal relaxed clock and the Yule speciation process. For tree calibration, we added to the alignment several species of Calopterygidae and two species of Amphipterygidae as outgroups (Supplementary Table 1). The crown node ages of these additional species were obtained from Dumont et al. (2005) and used as secondary calibrations: for *Hetaerina* we assigned a mean age of 60.1 million years ago (Mya) (SD = 1.2 Mya), for *Calopteryx* 21 Mya (SD = 3 Mya), for *Phaon* 31.9 Mya (SD = 3.4 Mya), for *Vestalis* 68.6 Mya (SD = 6.1 Mya), and for *Umma-Sapho* we used 53.1 Mya (SD = 2.1 Mya). Finally, we assigned a mean age of 151.5 Mya (SD = 5.8 Mya) for the divergence of Calopterygidae. A normal distribution was used for every calibration prior. We performed two independent runs with 200^6 of generations, sampling every 2000 generations. The convergence was evaluated in Tracer v. 1.7.0, and both runs were summarized using LogCombiner v. 1.8.4 and TreeAnnotator v. 1.8.4 (Drummond and Rambaut, 2007). All analyses were run on the CIPRES Science Gateway portal (Miller, 2010). A similar analysis was not conducted for the COI dataset because of the low resolution of the haplotype phylogeny.

2.4. Analyses of microsatellites

Microsatellites were analyzed in SPAGeDi v. 1.5 (Hardy and Vekemans, 2002) to estimate the mean number of alleles per locus (N_A), the mean effective number of alleles (N_{EA}), the rarefacted mean allelic richness ($AR_{K=2}$), and the average observed and expected heterozygosity (H_O and H_E, respectively). Deviations from Hardy-Weinberg equilibrium (HWE) were evaluated by calculating the inbreeding coefficient (F) and its significance in Arlequin v. 3.5.

A Bayesian clustering analysis was performed in STRUCTURE v. 2.3.4 (Pritchard et al., 2000), using the admixture model with correlated allele frequencies, without prior population information. The program was set to run with values of assumed genetic clusters (K) from 1 to 10 with a burn-in of 10,000 steps and chain length of 100,000. Ten independent runs were performed for each value of K. The most likely number of genetic clusters was determined using the method of Evanno (ΔK) (Evanno et al., 2005) in the STRUCTURE HARVESTER website (Earl and vonHoldt, 2012). Subsequent analyses in STRUCTURE were performed to assess substructure within the two main genetic clusters (see in Results) using similar program settings. Runs were summarized and plotted using CLUMPAK (Kopelman et al., 2015).

The magnitude of genetic differentiation among populations and among the genetic clusters identified in STRUCTURE were determined with analyses of molecular variance (AMOVA) in Arlequin v. 3.5 with 10,000 permutations.

2.5. Morphological data

To evaluate variation in the shape of the male caudal appendages we employed geometric morphometric techniques (Zelditch et al., 2004). We photographed the superior caudal appendages of 101 males under a stereoscopic microscope with a scale reference. On each image we superimposed a 'fan' on the right superior caudal appendage with the MakeFan v. 6 software (Zelditch et al., 2004) and then digitized six homologous points (i.e. landmarks *sensu* Bookstein, 1991) and 22 semilandmarks using the TpsDig v. 2 software (Rohlf, 2004). These landmarks and semilandmarks adequately describe the contour shape of the right superior caudal appendage in dorsal view (Supplementary Fig. 1). We performed a semilandmark superimposition using the Semiland module of Coordgen v.7 software (Zelditch et al., 2004) to minimize bending energy of the curves (Bookstein, 1991), and we also performed a superimposition Procrustes analysis using the CoordGen v. 7 software to evaluate appendage shape variation without the effect of size.

Principal component analyses (PCA) using Procrustes coordinates as shape variables were performed in PAST v. 3 (Hammer et al., 2001). We assigned the individuals to different nominal clusters based on the results of the genetic structure analysis for both nuclear and mitochondrial data. Shape variation in the caudal appendages between the different groups was visualized through a "thin-plate" analysis in Tgroup v. 7 software (Zelditch et al., 2004).

3. Results

3.1. Mitochondrial genetic diversity and neutrality tests

Two-hundred and sixteen sequences of the COI region were obtained and deposited at GenBank (see Supplementary Table 1 for accession numbers). In total, 61 haplotypes were observed with high haplotypic and nucleotide diversity (see Supplementary Table 3). The haplotype network based on statistical parsimony showed four major haplogroups (Fig. 1A). The first one (in green) included haplotype H9, which had the highest frequency (81 individuals), and other 26 haplotypes, which are singletons or have a low frequency and are separated from haplotype H9 by one to four mutational steps. This haplogroup was found in 20 populations from northern Mexico to Guatemala with different frequencies. This haplogroup is connected to a second haplogroup (in red; Fig. 1A) through ten mutational steps. In this second haplogroup there was also a central high frequency haplotype (H2, found in 40 individuals) and eighteen singletons. This haplogroup occurred in 19 populations with a distribution from Canada to northern Mexico. Another set of nine haplotypes (in blue in Fig. 1A), closely

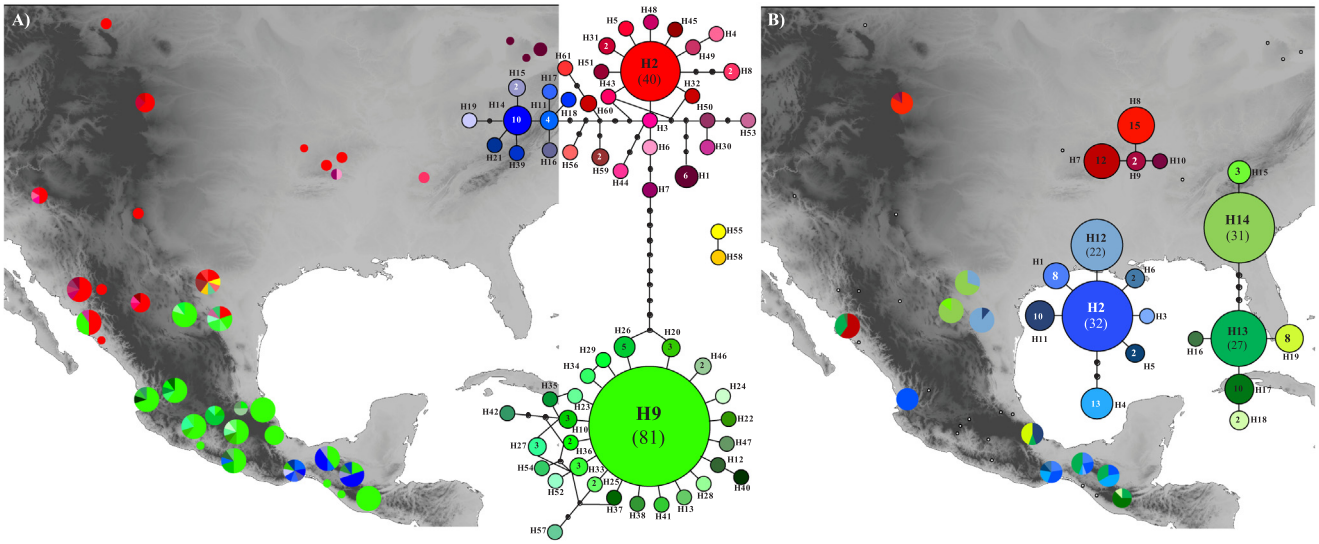

Fig. 1. Haplotype networks. (A) Geographic distribution and statistical parsimony network of 61 COI haplotypes of *H. americana*. (B) Geographic distribution and statistical parsimony network of 19 ITS haplotypes in a subsample of populations of *H. americana*. Pie charts represent frequencies of the haplotypes found in each sampling locality and the size of the chart is proportional to sample size. In the map, dark gray color represents higher altitudes. (For interpretation of the references to color in this figure legend, the reader is referred to the web version of this article.)

related to the red haplogroup, was found exclusively in four populations (20 individuals) of southern Mexico. Finally, two individuals from Zaragoza, Coahuila, harbored haplotypes (in yellow; Fig. 1A) that were a single mutational step from each other but disconnected from the rest of the network.

According to the AMOVA, genetic differentiation among populations was very high ($\Phi_{ST} = 0.65$, p-value < 0.0001). Differentiation among haplogroups was higher ($\Phi_{CT} = 0.89$, p-value < 0.0001) with also a considerable differentiation among populations within haplogroups ($\Phi_{SC} = 0.35$, p-value < 0.0001) and very high overall differentiation ($\Phi_{ST} = 0.93$, p-value < 0.0001) (Table 1).

The consensus phylogenetic tree based on haplotypes showed poor resolution, but the same four groups identified in the haplotype network can be distinguished (Fig. 2A). Nevertheless, the blue and red haplotypes did not form monophyletic clades, and the blue haplotypes appeared as basal. The yellow and green haplotypes formed a clade derived from the red group, with yellow haplotypes at the base (Fig. 2A).

In several populations the values of Tajima's D and Fu's Fs were negative and significant, suggesting a selective sweep or a recent population expansion. Furthermore, the d_N/d_S test for the whole dataset (Z-stat = −4.5; p-value < 0.0001) indicated deviation from neutrality, suggesting purifying selection acting on the COI gene. To further assess if this selection could be due to climatic differences among the geographic areas where the different haplogroups are distributed, we performed a principal components analysis on the values of the 19 bioclimatic variables corresponding to each population downloaded from the WorldClim database (Fick and Hijmans, 2017; http://www.worldclim.org/). The results are presented in Supplementary Fig. 2, with the populations corresponding to each of the haplogroups shown in their respective colors. The first component (PC1) explained 95.6% of the total variance and the second component (PC2) 3.6%, and mainly corresponded to temperature seasonality and annual precipitation, respectively. The climatic differentiation between the areas where the red and green + blue haplogroups occur is clear along the PC1 and was further supported by an ANOVA, performed with haplogroups as factors and population scores along the PC1 as dependent variable (F = 43.96, p-value < 0.0001). Meanwhile, the blue haplogroup was nested within the space of the green haplogroup.

3.2. Nuclear sequence variation and divergence times

For the ITS, we obtained 101 sequences (see Supplementary Table 1 for GenBank accession numbers), and after the phase and recombination analyses, a final alignment of 202 sequences with a length of 528 pb was used. In total, there were 19 haplotypes with high genetic diversity within populations and high positive and significant values of Tajima's D and Fu's Fs in some populations (Supplementary Table 4). The degree of population genetic differentiation according to the AMOVA was high ($\Phi_{ST} = 0.61$; p-value < 0.0001), as well as differentiation among haplogroups ($\Phi_{CT} = 0.92$, p-value < 0.0001) (Table 1). The haplotype network showed three disconnected haplogroups (Fig. 1B). The first haplogroup (in blue; Fig. 1B) was found distributed from southern (Chiapas) to northern Mexico (Coahuila) in seven populations with the most frequent haplotype in this haplogroup being H2 (17 individuals). The second haplogroup (in red; Fig. 1B) had only four haplotypes distributed in two populations in the north of Mexico (Sinaloa) and in the USA (Colorado). In this case, the most frequent haplotype was H8 (8 individuals). Finally, the third haplogroup (in green; Fig. 1B) had seven haplotypes present in seven populations from Guatemala to the northwest of Mexico, with two highly frequent haplotypes, H14 (16 individuals) and H13 (13 individuals). Most of the populations show a mixture of different haplogroups.

The consensus phylogenetic tree of ITS haplotypes showed three highly supported monophyletic clades (Fig. 2B) corresponding to the three haplogroups in the haplotype network. According to this tree, the red and the blue haplogroups are sister clades while the green haplogroup is basal to them. The BEAST dated tree (Fig. 3) suggests that the divergence between the blue + red and the green haplogroups was about 24.4 Mya (95% HPD 12.1–38.2 Mya; Fig. 3), and the divergence between the blue and the red clades was about 16.6 Mya (95% HPD 6.9–27.9 Mya).

3.3. Microsatellites genetic structure

Microsatellites showed low genetic diversity with a mean number of alleles per locus (N_A) from 1.0 to 3.0 across populations, and values of H_O and H_E between 0 and 0.37 and 0 and 0.55, respectively (Supplementary Table 5). Several populations showed deviations from HWE with high positive and significant *F* values, indicating a deficiency

Table 1
Analyses of molecular variance for COI and ITS sequences and for microsatellites. See text for details.

Loci	Group	Source of variation	d. f.	Sum of squares	Variance components	Percentage of variation	
COI	Global	Among populations	35	682.75	3.02	65.34	$\Phi_{ST} = 0.65^{**}$
		Within populations	180	288.38	1.6	34.66	
		Total	215	971.12	4.62		$\Phi_{ST} = 0.65^{**}$
	Haplogroups	Among groups	3	762.37	6.55	88.91	$\Phi_{CT} = 0.89^{**}$
		Among populations within groups	25	64.29	0.28	3.87	$\Phi_{SC} = 0.35^{**}$
		Within populations	176	93.6	0.53	7.22	
		Total	204	920.25	7.37		$\Phi_{ST} = 0.93^{**}$
ITS	Global	Among populations	10	1320.48	6.95	61.29	$\Phi_{ST} = 0.61^{**}$
		Within populations	191	838.98	4.39	38.71	
		Total	201	2159.47	11.35		$\Phi_{ST} = 0.61^{**}$
	Haplogroups	Among groups	3	1722.11	6.55	88.91	$\Phi_{CT} = 0.92^{**}$
		Among populations within groups	13	142.86	0.28	3.87	$\Phi_{SC} = 0.78^{**}$
		Within populations	186	46.78	0.53	7.22	
		Total	202	1911.75	7.36		$\Phi_{ST} = 0.98^{**}$
Microsatellites	Global	Among populations	23	181.61	0.43	51.16	$\Phi_{ST} = 0.51^{**}$
		Within populations	392	162.32	0.42	48.54	
		Total	415	343.94	0.85		$\Phi_{ST} = 0.51^{**}$
	Among genetic groups (K = 2)	Among groups	1	90.97	0.53	45.36	$\Phi_{CT} = 0.45^{**}$
		Among populations within groups	30	137.44	0.34	28.77	$\Phi_{SC} = 0.53^{**}$
		Within populations	384	115.52	0.3	26.86	
		Total	415	343.93	1.17		$\Phi_{ST} = 0.74^{**}$
	Among genetic groups (K = 2) for GG1	Among groups	1	74.9	0.5	50.4	$\Phi_{CT} = 0.50^{**}$
		Among populations within groups	24	24.56	0.05	5.19	$\Phi_{SC} = 0.10^{**}$
		Within populations	282	122.95	0.44	44.41	
		Total	307	222.41	0.99		$\Phi_{ST} = 0.56^{**}$
	Among genetic groups (K = 2) for GG2	Among groups	1	20.58	0.3	26.95	$\Phi_{CT} = 0.27^{*}$
		Among populations within groups	11	29.95	0.3	27.24	$\Phi_{SC} = 0.38^{**}$
		Within populations	95	47.88	0.5	45.63	
		Total	107	98.41	1.1		$\Phi_{ST} = 0.54^{**}$

d.f. = degrees of freedom. * = p-value $<$ 0.01; ** = p-value $<$ 0.0001.

of heterozygotes (Supplementary Table 5).

The STRUCTURE analysis supported the presence of two clearly delineated main genetic groups based on the ΔK method (K = 2; Fig. 4). The first genetic group (GG1) is mainly distributed from the United States to Chiapas in Southern Mexico. The second genetic group (GG2) was found in the population of Guatemala, two populations of Chiapas and the populations along the Gulf of Mexico coast and eastern Mexico plus a population in northwestern Mexico. It is important to mention that both genetic groups were found together in six populations (Fig. 4). In general, there was very little evidence of admixture between these two genetic groups. Individual assignments to one or the other genetic groups were higher than 90% in 95% of the cases and only 11 individuals showed evidence of mixed ancestry.

When we analyzed the substructure within each of these groups (Janes et al., 2017), we found two further subgroups within each of the two main groups (Supplementary Figs. 3 and 4). Within GG1 we found a genetic structure that strongly matched the latitudinal location of the populations (Supplementary Fig. 3). The first subgroup (GG1A) had a frequency higher than 90% in the United States and northern Mexico populations, and a lesser frequency (34 and 14%) in two central-western Mexico populations. The second subgroup (GG1B) was present mostly in central Mexico and southern populations. Only a few individuals (11) showed evidence of mixed ancestry between GG1A and GG1B, particularly in the population Chupícuaro in central-western Mexico. In the case of the second main genetic group (GG2) the analysis of substructure also revealed two subgroups (GG2A and GG2B) but with a less distinct geographical distribution and with higher levels of admixture (Supplementary Fig. 4).

The magnitude of genetic differentiation among populations was high ($\Phi_{ST} = 0.51$; p-value $<$ 0.0001) as well as the differentiation between the GG1 and GG2 main genetic groups ($\Phi_{CT} = 0.45$; p-value $<$ 0.0001) (Table 1). Differentiation between the GG1A and GG1B was similarly high ($\Phi_{ST} = 0.50$; p-value $<$ 0.0001), while differentiation between the GG2A and GG2B genetic groups was somewhat lower ($\Phi_{ST} = 0.27$; p-value $<$ 0.0001) (Table 1).

3.4. Morphological variation

The PCA based on the morphometric description of the shape of the superior caudal appendage revealed two clearly distinct morphological groups (Fig. 5). Remarkably, these two morphological groups perfectly matched the individual genetic assignment into the two main groups obtained in STRUCTURE, based on the nuclear microsatellites. It was also possible to observe a partial morphological differentiation between the GG1A and GG1B genetic subgroups (Fig. 5A). In contrast, there was no evidence of morphological differentiation between the GG2A and GG2B genetic subgroups. Also, there was no morphological differentiation corresponding to the COI haplogroups (Fig. 5B).

The deformation grids showed that the major variation between the two main morphological groups (GG1 and GG2) is in the median lobe and the distal part of the appendage. In the morphological group GG1, the median lobe is much flatter than the median lobe of group GG2, while the distal part of the appendage is shorter (Fig. 5B). Variation in shape between the genetic subgroups GG1A and GG1B was mainly in the median lobe (Fig. 5D).

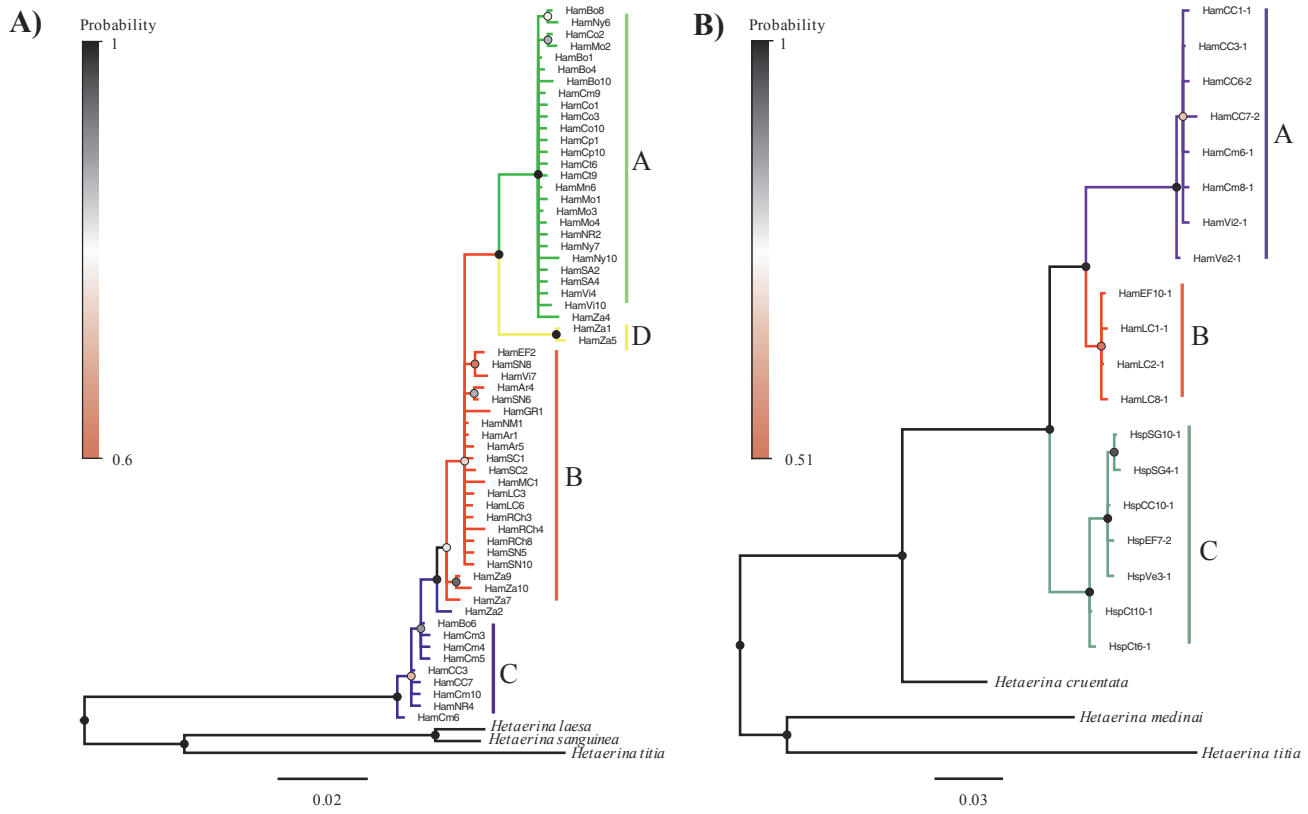

Fig. 2. Bayesian inference of haplotype relationships. (A) Gene tree of 61 haplotypes of the COI region. (B) Gene tree of 19 haplotypes of the ITS nuclear region. Bayesian posterior probability values are shown with colors in the node circles; the colors of the clades represent the different haplogroups found (see Fig. 1). (For interpretation of the references to color in this figure legend, the reader is referred to the web version of this article.)

4. Discussion

The results of this study show complex patterns of genetic and morphological variation within *H. americana*. Levels of genetic differentiation were very high for the three sets of molecular markers used (mitochondrial COI and nuclear ITS and microsatellites), but the COI variation was strongly discordant with the pattern shown by both nuclear markers. On the other hand, morphological variation in the male caudal appendages was completely congruent with nuclear genetic variation. Taken together, these results are consistent with recent views on speciation (Seehausen et al., 2014) and strongly suggest that *H. americana* is actually a complex of cryptic species at various stages of the speciation continuum

4.1. Mitonuclear discordance

There could be several explanations for incongruence between mitochondrial and nuclear genetic variation, including neutral demographic processes related to population history or differential dispersal and introgression patterns between the two sexes (since the mitochondria is maternally inherited). In our case, it also should be acknowledged that the number of nuclear sequences obtained was smaller than the number of COI sequences, therefore limiting a more detailed comparison between both datasets. However, the results of the d_N/d_S test strongly suggest that the COI region might be under purifying selection. This type of selection acting on mtDNA has been recurrently reported in many different animal species (Camus et al., 2017; Fontanillas et al., 2005; Quintela et al., 2014) and has been considered a feasible explanation for mitonuclear discordance (Morales et al., 2015). In most of these cases, the geographic distribution of haplotypes has been associated to temperature gradients (Fontanillas et al., 2005; Camus et al., 2017). Therefore, the influence of selection on the mitochondrial genome of the rubyspots studied here could also be the reason for the lack of congruence between the genealogical relationships between haplogroups and their geographic distribution, which is particularly clear in the case of the blue haplogroup, which is genealogically closer to the red haplotypes but overlaps in geographic distribution with the green haplotypes. This hypothesis is also supported by the significant climatic differences in temperature seasonality between the areas where the green + blue and the red haplotypes occur; but should be more carefully tested in further niche differentiation and ecophysiological studies.

4.2. Cryptic speciation in Hetaerina americana

In contrast to the mitochondrial DNA variation, the two sets of nuclear DNA markers (microsatellites and ITS sequences) were largely congruent with each other and with the morphological variation in the male caudal appendages. The main groups recognized (here called GG1 and GG2) were highly differentiated and showed little evidence of admixture even in sympatry. Remarkably, within each of these two main groups there was significant substructuring, detectable by both morphology and genetic variation, which was more pronounced within the GG1 than within the GG2. This evidence suggests that *H. americana* is a complex of biological entities at different degrees of divergence along the speciation continuum (i.e. from weakly reproductively isolated populations to irreversibly isolated species) (Seehausen et al., 2014), since we found three situations: (i) population groups with low genetic and morphological divergence (e. g. groups GG2A and GG2B), (ii) population groups with high genetic divergence and an incipient morphological divergence (GG1A and GG1B) and finally (iii) population groups with high genetic divergence and clear (i.e. non overlapping) morphological differentiation (GG1 and GG2).

The morphology of the caudal appendages is one of main sources of

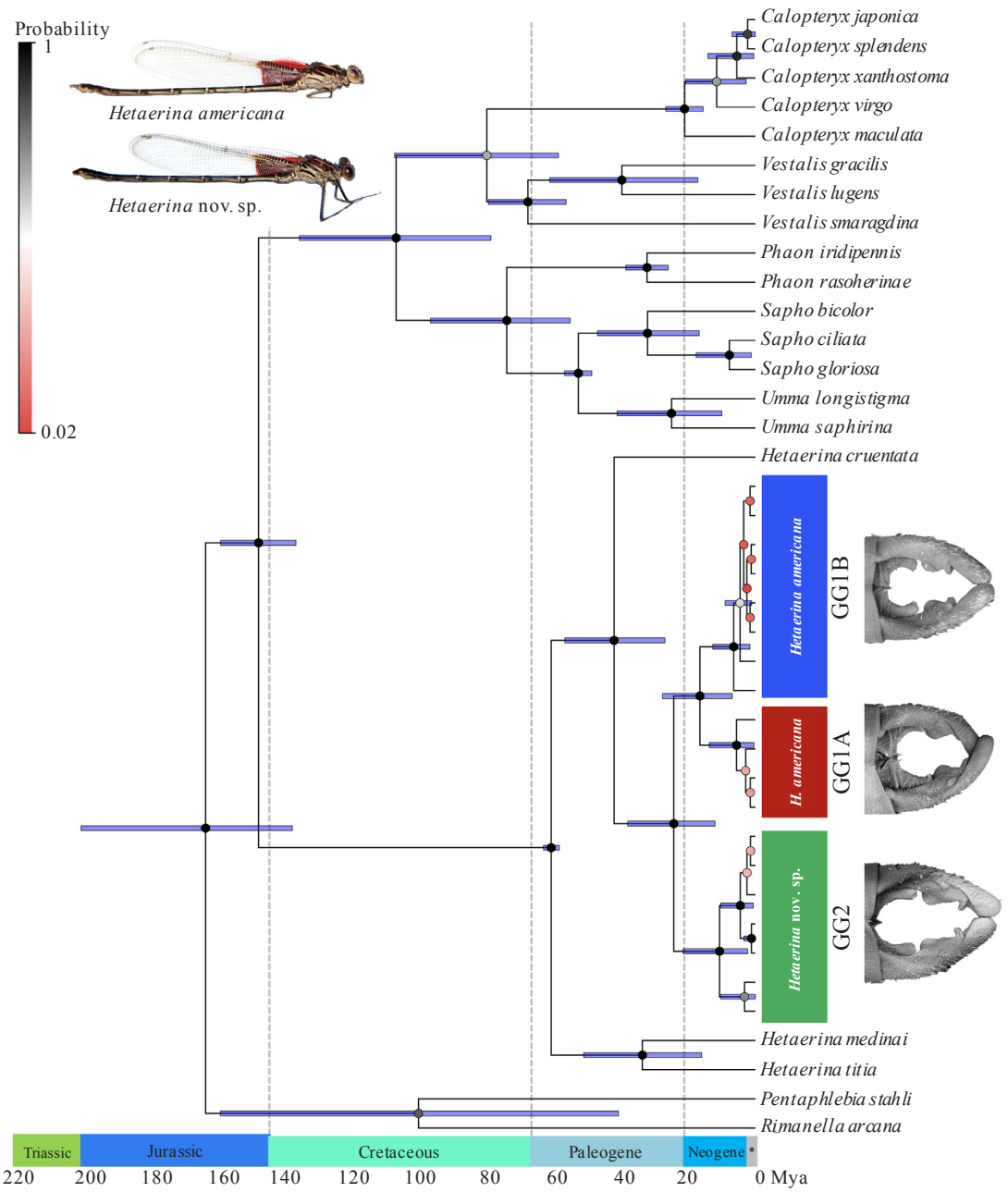

Fig. 3. Time calibrated tree based on ITS haplotypes. Bayesian posterior probabilities are shown with colors in the node circles. The node bars show the 95% Highest Posterior Density of node ages. The microsatellite genetic groups are signaled in their corresponding ITS clades. The morphological variation of caudal appendages is shown in electronic microscopic photographs (60 X) and the coloration pattern and morphology of male adults of *H. americana* and *H.* nov. sp. are illustrated. (For interpretation of the references to color in this figure legend, the reader is referred to the web version of this article.)

characters used by taxonomists for the recognition of species within some groups of Odonata, even in the case of phylogenetically closely related and ecologically similar lineages (such as in the genera *Ischnura* and *Enallagma*) (McPeek et al., 2011; Monetti et al., 2002). The divergence of these morphological structures is related to their important role in mate recognition during reproduction, functioning as a mechanical/sensory isolation mechanism (Barnard et al., 2017; Sánchez-Guillén et al., 2014). This role has been demonstrated through the experimental modification of these structures in *Enallagma* species, which results in the rejection of conspecific males by females (Robertson and Paterson, 1982). Thus, it has been suggested that mechanical/sensory isolation is, if not the most important, one of the main reproductive isolating barriers in odonates (Paulson, 1974).

Due to the variation found in the morphology of the caudal appendages in this study, and the congruence with the nuclear genetic groups, we can suggest that reproductive isolation exists even in localities where the groups occur in sympatry. This very low gene flow level is also evidenced by the minimal number of individuals that presented mixed ancestry (less than 10% of the sample). These results differ from those found in other odonates, for example, in the genus *Ischnura*, in which some of the taxonomically recognized species show low genetic differentiation related to high rates of hybridization (Sánchez-Guillén et al., 2011). This pattern is presumably observable when the divergence between species is recent and the species present incomplete reproductive barriers (Sánchez-Guillén et al., 2014, 2011). In contrast, in the case of the *H. americana* complex, the divergence among the genetic groups is probably old as observed in the dated phylogeny of the ITS haplotypes and suggested by the strong

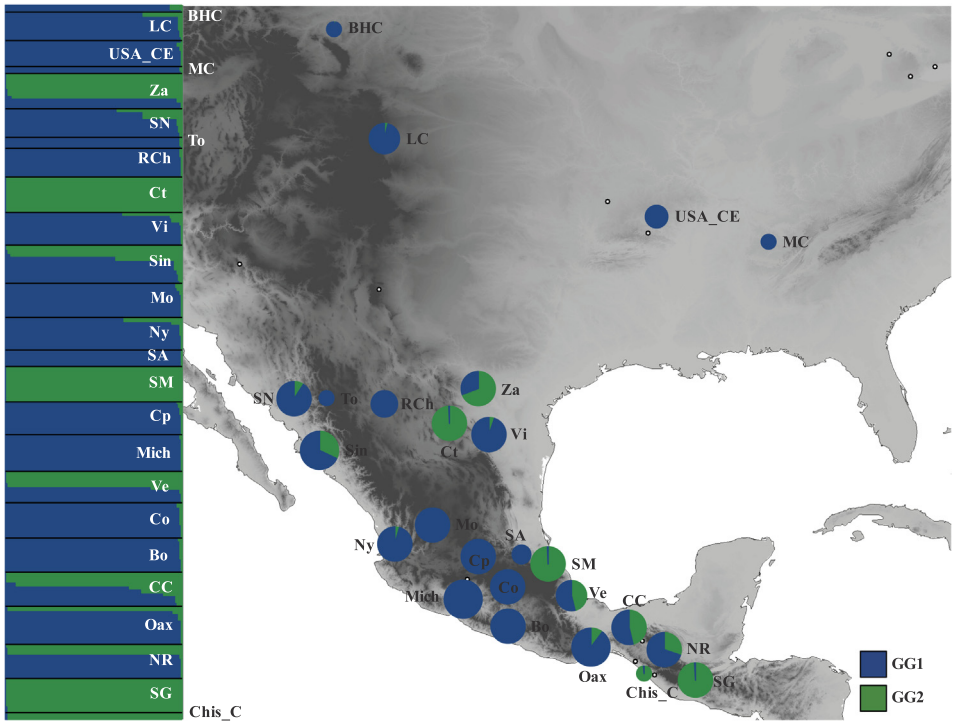

Fig. 4. STRUCTURE assignments for K = 2 in populations of *H. americana*. Individuals are represented by thin vertical lines, which are partitioned into K shaded segments representing each individual's estimated membership fraction; the black lines separate sampling sites. Pie charts represent the proportion and distribution of the two genetics groups in the populations. The size of pay charts represents the sample size analyzed. In the map, dark gray color represents higher altitudes. (For interpretation of the references to color in this figure legend, the reader is referred to the web version of this article.)

reproductive isolation. Even though divergence times should be taken with caution given the various possible sources of uncertainty, in general the results of our analysis are congruent with a recently published large time-calibrated phylogeny for all odonates (Waller and Svensson, 2017) in which and age of c.a. 60 my was also obtained for the divergence of the genus *Hetaerina*.

Overall, the results of this study allow us to propose that the *H. americana* complex includes, at least, two different cryptic species. The first one is *H. americana* Fabricius 1798, that shows the morphology described by Garrison (1990) and corresponds to the GG1, with a distribution from southern Mexico through almost the whole country to the United States (Colorado). The second species is *Hetaerina* nov. sp. that corresponds to the GG2 and presents a morphology of the superior caudal appendage that has not been described before (Fig. 3). This species is distributed from Guatemala to the north of Mexico but mostly along the Gulf of Mexico slope (but present in some populations in northwestern Mexico, what suggests that more extensive surveys are needed to clearly establish the geographic distribution of the two species). An interesting point is the stage of speciation between the GG1A and GG1B groups, which show morphological differentiation as well, but with a greater level of overlap between shapes, possibly related to a more recent divergence.

The detection of cryptic speciation is quite frequent (especially since the boom of molecular data) (Bickford et al., 2007). However, the evolutionary reasons for the retention of similar phenotypes among divergent lineages are not well understood (Fišer et al., 2018; Struck et al., 2018). Three main explanations have been suggested, which are recent divergence, morphological convergence and niche conservatism (Fišer et al., 2018). As previously mentioned, the first does not seem to be the case in the *H. americana* complex, given a probably old divergence and strong reproductive barriers. Second, the *H. americana* complex seems to be monophyletic according to the phylogenetic trees presented here and to a genus level phylogeny (unpublished data); thus, discarding the morphological convergence explanation. The last hypothesis, niche conservatism, seems more probable given the frequent sympatry between the GG1 and the GG2 and the lack of obvious differentiation in climatic niche across their distribution. The result of this conservatism could be a constrained evolution of external morphological features (as body size, shape and coloration), from processes such as stabilizing selection. In this way, by selecting against extreme phenotypic traits, stabilizing selection prevents morphological divergence, and distinct populations will remain similar over long periods of time (Fišer et al., 2018; Smith et al., 2011). In fact, it has been suggested that the process of diversification in zygopterans is mainly "non-adaptive", that is, occurs most often through non-ecological speciation (Rundell and Price, 2009; Czekanski-Moir and Rundell, 2019). This is because niche conservatism is common among closely related damselfly species and divergence is generally associated to traits involved in mate recognition system, such as coloration and the shape of the caudal appendages, which are traits whose evolution is usually driven by sexual selection (Wellenreuther and Sánchez-Guillén, 2016).

Acknowledgements

We thank Eliot Camacho, Ricardo Durán, Mariana Solís, Luis Letelier, Aly Valderrama, Sergio Marcos, Gonzalo Contreras, Elsa Hernández, Hernando Rodríguez and Tamara Ochoa for helping in field collection. We especially thank George Sims for sending us samples from USA. Jesús Llanderal and Víctor Rocha provided technical help with microsatellites sequencing and Orlando Hernández for the microscopy photographs of caudal appendages. Y. M. Vega-Sánchez thanks CONACyT (CVU 549239) and the Posgrado en Ciencias Biológicas – UNAM for providing funding and facilities to develop graduate studies at UNAM. This article constitutes a partial fulfillment of the graduate program in Biological Sciences of UNAM.

Funding source

This work was supported by the grant number MICH-2012-C05-197824, Fondos Mixtos CONACYT-Gobierno del Estado de Michoacán.

Appendix A. Supplementary material

Supplementary data to this article can be found online at https://doi.org/10.1016/j.ympev.2019.106536.

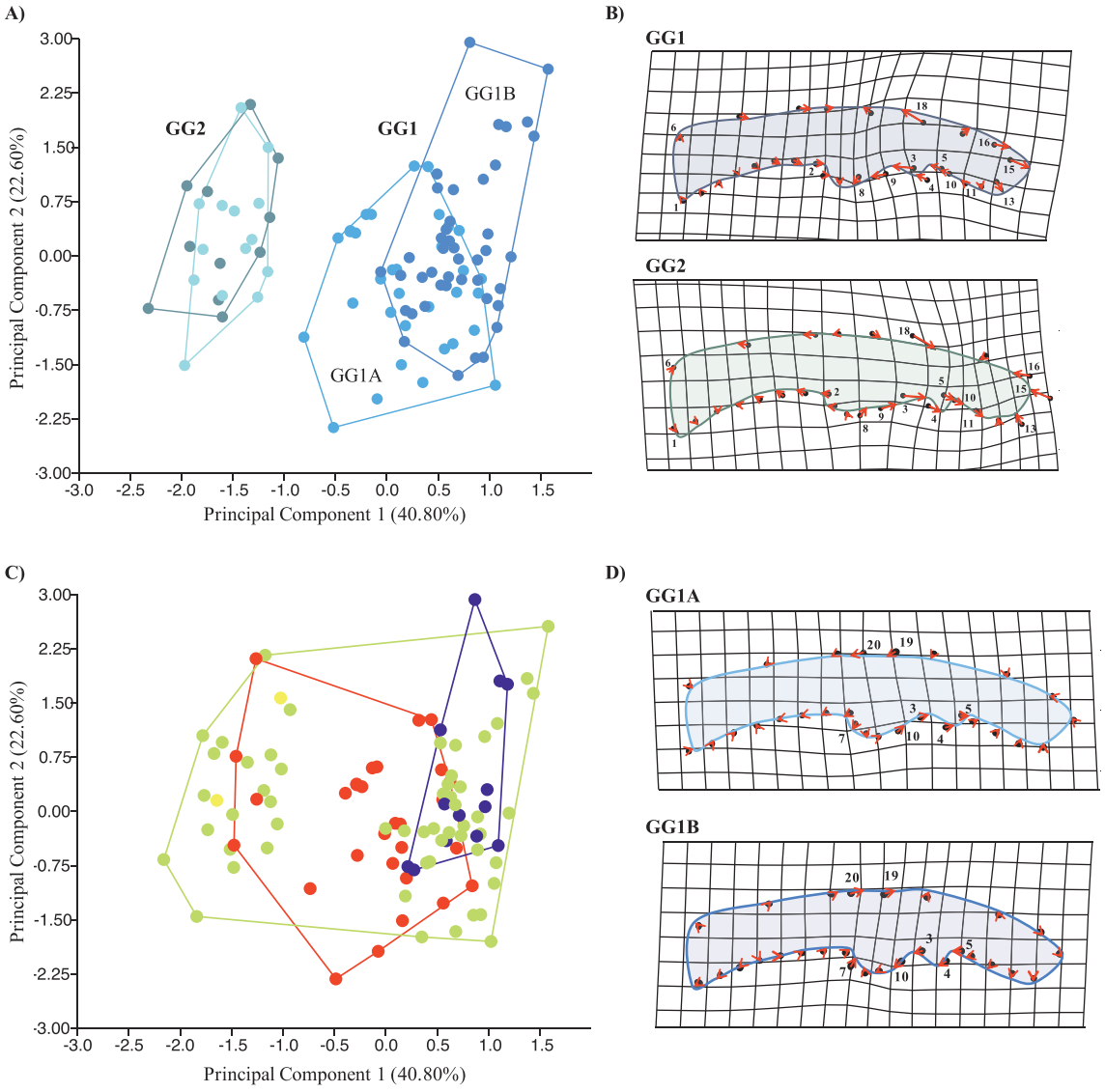

Fig. 5. Differences in shape of the superior caudal appendage. (A) Principal components analysis based on the coordinates that describe the shape of the superior caudal appendage; the color of the circles represents the nuclear genetic group based on microsatellites. (B) Superior caudal appendage shapes: deformation grids represent the mean shape for each morphological-nuclear genetic group; the size and direction of the arrows represent the deformation degree of each morphological group with respect to each other. (C) Principal component analysis; the color of the circles represents the mitochondrial (COI) haplogroups. (D) Superior caudal appendage shapes: deformation grids represent the mean shape for each morphological-nuclear genetic subgroup (GG1A and GG1B); the size and direction of the arrows represent the deformation degree of each morphological group with respect to the other. (For interpretation of the references to color in this figure legend, the reader is referred to the web version of this article.)

References

Anderson, C.N., Grether, G.F., 2013. Characterization of novel microsatellite loci for *Hetaerina americana* damselflies, and cross-amplification in other species. Conserv. Genet. Resour. 5, 149–151. https://doi.org/10.1007/s12686-012-9755-x.

Avise, J.C., 2000. Phylogeography: The History and Formation of Species. Harvard University Press, Cambridge.

Barnard, A.A., Fincke, O.M., McPeek, M.A., Masly, J.P., 2017. Mechanical and tactile incompatibilities cause reproductive isolation between two young damselfly species. Evol. 71, 2410–2427. https://doi.org/10.1111/evo.13315.

Battin, T.J., 1993. The odonate mating system, communication, and sexual selection: a review. Bolletino di zoologia 60, 353–360. https://doi.org/10.1080/11250009309355839.

Bickford, D., Lohman, D.J., Sodhi, N.S., Ng, P.K.L., Meier, R., Winker, K., Ingram, K.K., Das, I., 2007. Cryptic species as a window on diversity and conservation. Trends Ecol. Evol. 22, 148–155. https://doi.org/10.1016/j.tree.2006.11.004.

Bookstein, F.L., 1991. Morphometric Tools for Landmark Data: Geometry and Biology. Cambridge University Press, New York.

Bouckaert, R., Heled, J., Kühnert, D., Vaughan, T., Wu, C.-H., Xie, D., Suchard, M.A., Rambaut, A., Drummond, A.J., 2014. BEAST 2: A software platform for Bayesian evolutionary analysis. PLoS Comput. Biol. 10, e1003537. https://doi.org/10.1371/journal.pcbi.1003537.

Callahan, M.S., McPeek, M.A., 2016. Multi-locus phylogeny and divergence time estimates of *Enallagma* damselflies (Odonata: Coenagrionidae). Mol. Phyl. Evol. 94, 182–195. https://doi.org/10.1016/j.ympev.2015.08.013.

Camus, M.F., Wolff, J.N., Sgrò, C.M., Dowling, D.K., 2017. Experimental support that natural selection has shaped the latitudinal distribution of mitochondrial haplotypes in australian *Drosophila melanogaster*. Mol. Biol. Evol. 34, 2600–2612. https://doi.org/10.1093/molbev/msx184.

Clement, M., Posada, D., Crandall, K.A., 2000. TCS: A computer program to estimate gene genealogies. Mol. Ecol. 9, 1657–1659. https://doi.org/10.1046/j.1365-294X.2000.01020.x.

Contreras-Garduño, J., Buzatto, B.A., Serrano-Meneses, M.A., Nájera-Cordero, K., Córdoba-Aguilar, A., 2008. The size of the red wing spot of the American rubyspot as a heightened condition-dependent ornament. Behav. Ecol. 19, 724–732. https://doi.org/10.1093/beheco/arn026.

Corbet, P.S., 1962. A Biology of Dragonflies, first ed. Witherby, London.

Córdoba-Aguilar, A., Raihani, G., Serrano-Meneses, M.A., Contreras-Garduño, J., 2009. The lek mating system of *Hetaerina* damselflies (Insecta: Calopterygidae). Behaviour 146, 189–207. https://doi.org/10.1163/156853909X410739.

Czekanski-Moir, J.E., Rundell, R.J., 2019. The ecology of nonecological speciation and nonadaptive radiations. TREE 34, 400–415. https://doi.org/10.1016/j.tree.2019.01.012.

Darriba, D., Taboada, G.L., Doallo, R., Posada, D., 2012. JModelTest 2: More models, new

heuristics and parallel computing. Nat. Methods 9, 772. https://doi.org/10.1038/nmeth.2109.
Dijkstra, K.-D.B., Kalkman, V.J., Dow, R.A., Stokvis, F.R., van Tol, J., 2014. Redefining the damselfly families: a comprehensive molecular phylogeny of Zygoptera (Odonata). Syst. Entomol. 39, 68–96. https://doi.org/10.1111/syen.12035.
Drummond, A.J., Rambaut, A., 2007. BEAST: Bayesian evolutionary analysis by sampling trees. BMC Evol. Biol. 7, 214. https://doi.org/10.1186/1471-2148-7-214.
Dumont, H.J., Vanfleteren, J.R., De Jonckheere, J.F., Weekers, P.H., 2005. Phylogenetic relationships, divergence time estimation, and global biogeographic patterns of calopterygoid damselflies (Odonata, Zygoptera) inferred from ribosomal DNA sequences. Syst. Biol. 54, 347–362. https://doi.org/10.1080/10635150590949869.
Dumont, H.J., Vierstraete, A., Vanfleteren, J.R., 2010. A molecular phylogeny of the Odonata (Insecta). Syst. Entomol. 35, 6–18. https://doi.org/10.1111/j.1365-3113.2009.00489.x.
Earl, D.A., vonHoldt, B.M., 2012. STRUCTURE HARVESTER: a website and program for visualizing STRUCTURE output and implementing the Evanno method. Conserv. Genet. Resour. 4, 359–361. https://doi.org/10.1007/s12686-011-9548-7.
Evanno, G., Regnaut, S., Goudet, J., 2005. Detecting the number of clusters of individuals using the software STRUCTURE: a simulation study. Mol. Ecol. 14, 2611–2620. https://doi.org/10.1111/j.1365-294X.2005.02553.x.
Excoffier, L., Lischer, H.E., 2010. Arlequin suite ver 3.5: a new series of programs to perform population genetics analyses under Linux and Windows. Mol. Ecol. Resour. 10, 564–567. https://doi.org/10.1111/j.1755-0998.2010.02847.x.
Feindt, W., Fincke, O.M., Hadrys, H., 2014. Still a one species genus? Strong genetic diversification in the world's largest living odonate, the Neotropical damselfly *Megaloprepus caerulatus*. Conserv. Genet. 15, 469–481. https://doi.org/10.1007/s10592-013-0554-z.
Ferreira, S., Boudot, J.-P., Haissoufi, M. El, Alves, P.C., Thompson, D.J., Brito, J.C., Watts, P.C., 2016. Genetic distinctiveness of the damselfly *Coenagrion puella* in North Africa: an overlooked and endangered taxon. Conserv. Genet. 17, 985–991. https://doi.org/10.1007/s10592-016-0826-5.
Fick, S.E., Hijmans, R.J., 2017. Worldclim 2: new 1-km spatial resolution climate surfaces for global land areas. Int. J. of Climatol. 37, 4302–4315. https://doi.org/10.1002/joc.5086.
Fincke, O.M., Xu, M., Khazan, E.S., Wilson, M., Ware, J.L., 2018. Tests of hypotheses for morphological and genetic divergence in *Megaloprepus* damselflies across Neotropical forests. Biol. J. Linn. Soc. 277, 549. https://doi.org/10.1093/biolinnean/bly148.
Fišer, C., Robinson, C.T., Malard, F., 2018. Cryptic species as a window into the paradigm shift of the species concept. Mol. Ecol. 27, 613–635. https://doi.org/10.1111/mec.14486.
Fontanillas, P., Dépraz, A., Giorgi, M.S., Perrin, N., 2005. Nonshivering thermogenesis capacity associated to mitochondrial DNA haplotypes and gender in the greater white-toothed shrew, *Crocidura russula*. Mol. Ecol. 14, 661–670. https://doi.org/10.1111/j.1365-294X.2004.02414.x.
Futuyma, D.J., Kirkpatrick, M., 2017. Evolution, fourth ed. Sinauer, Massachusetts.
Garrison, R.W., 1990. A synopsis of the genus *Hetaerina* with descriptions of four new species (Odonata: Calopterygidae). Trans. Am. Entomol. Soc. 1890 (116), 175–259. https://doi.org/10.2307/25078514.
Grether, G.F., 1996. Sexual selection and survival selection on wing coloration and body size in the Rubyspot damselfly *Hetaerina americana*. Evol. 50, 1939–1948. https://doi.org/10.2307/2410752.
Hammer, Ø., Harper, D.A.T., Ryan, P.D., 2001. PAST: paleontological statistics software package for education and data analysis. Palaeontologia Electronica 4, 1.
Hardy, O.J., Vekemans, X., 2002. SPAGeDI: A versatile computer program to analyse spatial genetic structure at the individual or population levels. Mol. Ecol. Notes 2, 618–620. https://doi.org/10.1046/j.1471-8286.2002.00305.x.
Hayashi, F., Dobata, S., Futahashi, R., 2005. Disturbed population genetics: suspected Introgressive hybridization between two *Mnais* damselfly species (Odonata). Zoolog. Sci. 22, 869–881. https://doi.org/10.2108/zsj.22.869.
Janes, J.K., Miller, J.M., Dupuis, J.R., Malenfant, R.M., Gorrell, J.C., Cullingham, C.I., Andrew, R.L., 2017. The K= 2 conundrum. Mol. Ecol. 26, 3594–3602. https://doi.org/10.1111/mec.14187.
Jones, B.R., Jordan, S., 2015. Genetic consequences of Pleistocene sea-level change on Hawaiian *Megalagrion* damselflies. J. Hered. 106, 618–627. https://doi.org/10.1093/jhered/esv036.
Jukes, T.H., Cantor, C.R., 1969. Evolution of protein molecules. In: Mammalian Protein Metabolism. Academic Press, New York.
Kohli, M.K., Sahlén, G., Kuhn, W.R., Ware, J.L., 2018. Extremely low genetic diversity in a circumpolar dragonfly species, *Somatochlora sahlbergi* (Insecta: Odonata: Anisoptera). Sci. Rep. 8, 15114. https://doi.org/10.1038/s41598-018-32365-7.
Kopelman, N.M., Mayzel, J., Jakobsson, M., Rosenberg, N.A., Mayrose, I., 2015. Clumpak: a program for identifying clustering modes and packaging population structure inferences across K. Mol. Ecol. Resour. 15, 1179–1191. https://doi.org/10.1111/1755-0998.12387.
Kumar, S., Stecher, G., Li, M., Knyaz, C., Tamura, K., 2018. MEGA X: molecular evolutionary genetics analysis across computing platforms. Mol. Biol. Evol. 35, 1547–1549. https://doi.org/10.1093/molbev/msy096.
Librado, P., Rozas, J., 2009. DnaSP v5: a software for comprehensive analysis of DNA polymorphism data. Bioinformatics 25, 1451–1452. https://doi.org/10.1093/bioinformatics/btp187.
McPeek, M.A., Symes, L.B., Zong, D.M., McPeek, C.L., 2011. Species recognition and patterns of population variation in the reproductive structures of a damselfly genus. Evol. 65, 419–428. https://doi.org/10.1111/j.1558-5646.2010.01138.x.
Miller, M.A., 2010. Creating the CIPRES science gfor inference of large phylogenetic trees. In: Proceedings of the Gateway Computing Environments Workshop (GCE), New Orleans, LA. pp. 1–8. doi: 10.1109/GCE.2010.5676129.
Monetti, L., Sánchez-Guillén, R.A., Cordero-Rivera, A., 2002. Hybridization between *Ischnura graellsii* (Vander Linder) and *I. elegans* (Rambur) (Odonata: Coenagrionidae): are they different species? Biol. J. Linn. Soc. 76, 225–235. https://doi.org/10.1046/j.1095-8312.2002.00060.x.
Morales, H.E., Pavlova, A., Joseph, L., Sunnucks, P., 2015. Positive and purifying selection in mitochondrial genomes of a bird with mitonuclear discordance. Mol. Ecol. 24, 2820–2837. https://doi.org/10.1111/mec.13203.
Nava-Bolaños, A., Sánchez-Guillén, R.A., Munguía-Steyer, R.E., Córdoba-Aguilar, A., 2016. Isolation barriers and genetic divergence in non-territorial *Argia* damselflies. Biol. J. Linn. Soc. 180, 804–817. https://doi.org/10.1111/bij.12916.
Nei, M., Gojobori, T., 1986. Simple methods for estimating the numbers of synonymous and nonsynonymous nucleotide substitutions. Mol. Biol. Evol. 3, 418–426. https://doi.org/10.1093/oxfordjournals.molbev.a040410.
Paulson, D.R., 1974. Reproductive isolation in damselflies. Syst. Zool. 23, 40–49.
Pritchard, J.K., Stephens, M., Donnelly, P., 2000. Inference of population structure using multilocus genotype data. Genetics 155, 945–959.
Quintela, M., Johansson, M.P., Kristjánsson, B.K., Barreiro, R., Laurila, A., 2014. AFLPs and mitochondrial haplotypes reveal local adaptation to extreme thermal environments in a freshwater gastropod. PLoS ONE 9, e101821. https://doi.org/10.1371/journal.pone.0101821.
Raihani, G., Serrano-Meneses, M.A., Córdoba-Aguilar, A., 2008. Male mating tactics in the American rubyspot damselfly: territoriality, nonterritoriality and switching behaviour. Anim. Behav. 75, 1851–1860. https://doi.org/10.1016/j.anbehav.2007.11.002.
Rambaut, A., Drummond, A.J., Xie, D., Baele, G., Suchard, M.A., 2018. Posterior summarisation in Bayesian phylogenetics using Tracer 1.7. Syst. Biol. 67, 901–904. https://doi.org/10.1093/sysbio/syy032.
Robertson, H.M., Paterson, H.E.H., 1982. Mate recognition and mechanical isolation in *Enallagma* damselflies (Odonata: Coenagrionidae). Evol. 36, 243. https://doi.org/10.2307/2408042.
Rohlf, F.J., 2004. tpsDig, Digitize Landmarks and Outlines v. 2.0. Department of Ecology and Evolution, State University of New York at Stony Brook.
Ronquist, F., Teslenko, M., Van Der Mark, P., Ayres, D.L., Darling, A., Höhna, S., Larget, B., Liu, L., Suchard, M.A., Huelsenbeck, J.P., 2012. Mrbayes 3.2: efficient bayesian phylogenetic inference and model choice across a large model space. Syst. Biol. 61, 539–542. https://doi.org/10.1093/sysbio/sys029.
Rundell, R.J., Price, T.D., 2009. Adaptive radiation, nonadaptive radiation, ecological speciation and nonecological speciation. TREE 24, 394–399. https://doi.org/10.1016/j.tree.2009.02.007.
Sánchez-Guillén, R.A., Córdoba-Aguilar, A., Cordero-Rivera, A., Wellenreuther, M., 2014a. Genetic divergence predicts reproductive isolation in damselflies. J. Evol. Biol. 27, 76–87. https://doi.org/10.1111/jeb.12274.
Sánchez-Guillén, R.A., Córdoba-Aguilar, A., Cordero-Rivera, A., Wellenreuther, M., 2014b. Rapid evolution of prezygotic barriers in non-territorial damselflies. Biol. J. Linn. Soc. 113, 485–496. https://doi.org/10.1111/bij.12347.
Sánchez-Guillén, R.A., Wellenreuther, M., Cordero-Rivera, A., Hansson, B., 2011. Introgression and rapid species turnover in sympatric damselflies. BMC Evol. Biol. 11, 210. https://doi.org/10.1186/1471-2148-11-210.
Sánchez-Herrera, M., Realpe, E., Salazar, C., 2010. A neotropical polymorphic damselfly shows poor congruence between genetic and traditional morphological characters in Odonata. Mol. Phyl. Evol. 57, 912–917. https://doi.org/10.1016/j.ympev.2010.08.016.
Seehausen, O., Butlin, R.K., Keller, I., Wagner, C.E., Boughman, J.W., Hohenlohe, P.A., Peichel, C.L., Saetre, G.-P., Bank, C., Brännström, Å., Brelsford, A., Clarkson, C.S., Eroukhmanoff, F., Feder, J.L., Fischer, M.C., Foote, A.D., Franchini, P., Jiggins, C.D., Jones, F.C., Lindholm, A.K., Lucek, K., Maan, M.E., Marques, D.A., Martin, S.H., Matthews, B., Meier, J.I., Möst, M., Nachman, M.W., Nonaka, E., Rennison, D.J., Schwarzer, J., Watson, E.T., Westram, A.M., Widmer, A., 2014. Genomics and the origin of species. Nat. Rev. Genet. 15, 176–192. https://doi.org/10.1038/nrg3644.
Smith, K.L., Harmon, L.J., Shoo, L.P., Melville, J., 2011. Evidence of constrained phenotypic evolution in a cryptic species complex of agamid lizards. Evol. 65, 976–992. https://doi.org/10.1111/j.1558-5646.2010.01211.x.
Struck, T.H., Feder, J.L., Bendiksby, M., Birkeland, S., Cerca, J., Gusarov, V.I., Kistenich, S., Larsson, K.-H., Liow, L.H., Nowak, M.D., Stedje, B., Bachmann, L., Dimitrov, D., 2018. Finding evolutionary processes hidden in cryptic species. Trends Ecol. Evol. 33, 153–163. https://doi.org/10.1016/j.tree.2017.11.007.
Svensson, E.I., Kristoffersen, L., Oskarsson, K., Bensch, S., 2004. Molecular population divergence and sexual selection on morphology in the banded demoiselle (*Calopteryx splendens*). Heredity 93, 423–433. https://doi.org/10.1038/sj.hdy.6800519.
Svensson, E.I., Nordén, A., Waller, J.T., Runemark, A., 2016. Linking intra- and interspecific assortative mating: Consequences for asymmetric sexual isolation. Evol. 70, 1165–1179. https://doi.org/10.1111/evo.12939.
Svensson, E.I., Waller, J.T., 2013. Ecology and sexual selection: evolution of wing pigmentation in calopterygid damselflies in relation to latitude, sexual dimorphism, and speciation. Am. Nat. 182, E174–E195. https://doi.org/10.1086/673206.
Swaegers, J., Janssens, S.B., Ferreira, S., Watts, P.C., Mergeay, J., McPeek, M.A., Stoks, R., 2014. Ecological and evolutionary drivers of range size in *Coenagrion* damselflies. J. Evol. Biol. 27, 2386–2395. https://doi.org/10.1111/jeb.12481.
Troast, D., Suhling, F., Jinguji, H., Sahlén, G., Ware, J.L., 2016. A global population genetic study of *Pantala flavescens*. PLoS ONE 11, e0148949–e149013. https://doi.org/10.1371/journal.pone.0148949.
Tynkkynen, K., Grapputo, A., Kotiaho, J.S., Rantala, M.J., Väänänen, S., Suhonen, J., 2008. Hybridization in *Calopteryx* damselflies: the role of males. Anim. Behav. 75, 1431–1439. https://doi.org/10.1016/j.anbehav.2007.09.017.
Vega-Sánchez, Y.M., 2013. Análisis cladístico, genético y morfológico del género *Hetaerina*. Thesis. Universidad Michoacana de San Nicolás de Hidalgo, Morelia,

Michoacán. Mexico.
Waller, J.T., Svensson, E., 2017. Body size evolution in an old insect order: no evidence for Cope's Rule in spite of fitness benefits of large size. Evolution 71, 2178–2193 10.1111/evo.13302.
Watts, P.C., Rouquette, J.R., Saccheri, I.J., Kemp, S.J., Thompson, D.J., 2004. Molecular and ecological evidence for small-scale isolation by distance in an endangered damselfly, *Coenagrion mercuriale*. Mol. Ecol. 13, 2931–2945. https://doi.org/10.1111/j.1365-294X.2004.02300.x.
Weekers, P.H.H., De Jonckheere, J.F., Dumont, H.J., 2001. Phylogenetic relationships inferred from ribosomal its sequences and biogeographic patterns in representatives of the genus *Calopteryx* (Insecta: Odonata) of the West Mediterranean and adjacent West European zone. Mol. Phyl. Evol. 20, 89–99. https://doi.org/10.1006/mpev.2001.0947.
Wellenreuther, M., Sánchez-Guillén, R.A., 2016. Nonadaptive radiation in damselflies. Evol. Appl. 9, 103–118. https://doi.org/10.1111/eva.12269.
Woerner, A.E., Cox, M.P., Hammer, M.F., 2007. Recombination-filtered genomic datasets by information maximization. Bioinformatics 23, 1851–1853. https://doi.org/10.1093/bioinformatics/btm253.
Zelditch, M., Swiderski, D., Sheets, H., Fink, W., 2004. Geometric Morphometrics for Iologists, first ed. Elsevier doi:10.1016/B978-0-12-778460-1.X5000-5.